Supplementary Figure 1. Hemorrhagic shock causes hepatic injury and affects the expression and activity of DMEs.

(A) Liver histology of WT mice subject to sham surgery or HS/R was analyzed by H&E staining. The "N"s within the dotted circle indicate the necrotic areas. **(B)** Apoptosis was analyzed by TUNEL staining. CV, central vein. **(C)** The hepatic expression of Cyp3a11 was measured by immunostaining. **(D)** Mice are the same as in (A). Shown are the serum levels of ALT. **(E)** The hepatic gene expression was measured by qRT-PCR. **(F)** The hepatic expression of Cyp3a11 was measured by Western blotting. **(G)** Schematic presentation of midazolam metabolism by CYP3A4 in human and Cyp3a11 in mice (left). The liver microsomal formation of 1'-OH midazolam was measured by UPLC-MS (right). **(H)** Schematic presentation of oxycodone metabolism by CYP3A4 in human (Cyp3a11 in mice) and CYP2D6 in human (Cyp2d22 in mice) (left). The liver microsomal formations of noroxycodone and oxymorphone were measured by UPLC-MS (right). **(I)** The hepatic gene expression was measured by qRT-PCR in WT mice subject to sham surgery or HS without resuscitation. **(J)** Mice are the same as in (H). The hepatic protein expression of Cyp3a11 was measured by Western blotting. Results are presented as mean ±SE. n=4~5 for each group. *, $p < 0.05$; **, $p < 0.01$, compared to the sham groups.

Supplementary Figure 2. Treatment with DEX sensitizes mice to HS-induced hepatic injury in a PXR-dependent manner. (A) Schematic representation of the DEX pre-treatment model. WT and $Pxr^{-/-}$ mice were intraperitoneally injected with DEX (20 mg/kg per day) for two days before receiving the sham surgery or HS/R. **(B)** The hepatic mRNA expression of *Cyp3a11* was measured by qRT-PCR. **(C)** Liver histology was analyzed by H&E staining. Bar is 100 μm.

(D-F) Mice are the same as in (C). Shown are quantification of necrotic areas (D), Suzuki scores (E), and serum levels of ALT (F) in mice subject to HS/R. Results are presented as mean ±SE. n=4~5 for each group. *, $p < 0.05$; **, $p < 0.01$, the comparisons are labeled (B and F), or compared to WT+VEH (D and E).

Supplementary Figure 3. Treatment with the CAR agonist TCPOBOP fails to sensitize mice to HS-induced hepatic injury. (A) Schematic representation of the TCPOBOP pre-treatment model. WT mice were intraperitoneally injected with TCPOBOP (0.25 mg/kg per day) for three days before receiving the sham surgery or HS/R. **(B)** The hepatic mRNA expression of *Cyp2b10* was measured by qRT-PCR. **(C)** Liver histology was analyzed by H&E staining. Bar is 100 μm. **(D and E)** Mice are the same as in (C). Shown are quantification of necrotic areas (D) and Suzuki scores (E). Results are presented as mean ±SE. n=4~5 for each group. *, $p < 0.05$; **, $p < 0.01$, the comparisons are labeled.

Supplementary Figure 4. Post-hemorrhagic shock treatment of CYP3A inhibitor KET attenuates HS-induced hepatic injury. (A) The hepatic mRNA expression of *Cyp3a11* at indicated time points after HS was measured by qRT-PCR. **(B)** Schematic representation of the KET post-HS treatment model. WT mice were intraperitoneally injected with PCN (40 mg/kg) or VEH for two days before receiving the sham surgery or HS/R. KET (95 mg/kg) or VEH was given either 2-h after the initiation of HS (at 72 h), or 12-h after the initiation of HS (at 84 h). **(C)** Liver histology was analyzed by H&E staining. Bar is 100 μm. **(D-F)** Mice are the same as in (C). Shown are quantification of necrotic areas (D), Suzuki scores (E), and serum ALT levels

(F). Results are presented as mean ±SE. n=3 for each group. *, $p < 0.05$; **, $p < 0.01$, compared to VEH (D and E), or the comparisons are labeled (F).

Supplementary Figure 5. Ablation of Cyp3a abolishes the sensitizing effect of PCN. (A) PCR genotying to validate the creation of VP-PXR/Cyp3a$^{-/-}$ mice. **(B)** The hepatic mRNA expression of *Cyp3a11* and *Cyp2b10* was measured by qRT-PCR. **(C)** Liver histology was analyzed by H&E staining in PCN-treated WT and Cyp3a$^{-/-}$ mice subject to sham surgery or HS/R. Bar is 100 μm. **(D-F)** Mice are the same as in (C). Shown are quantification of necrotic areas (D), Suzuki scores (E), and serum levels of ALT (F) in mice subject to HS/R. Results are presented as mean ±SE. n=3 for each group. *, $p < 0.05$; **, $p < 0.01$, compared to WT.

Supplementary Figure 6. Treatment with the antioxidant NACA attenuates the sensitizing effect of PCN and DEX on HS-induced hepatic injury. WT mice were treated with PCN or DEX, in the absence or presence of NACA, before receiving the sham surgery or HS/R. **(A)** Liver histology was analyzed by H&E staining. Bar is 100 μm. **(B)** Serum levels of ALT. Results are presented as mean ±SE. n=4 for each group. *, $p < 0.05$; **, $p < 0.01$, the comparisons are labeled.

Supplementary Figure 7. Co-treatment of the VP-PXR transgenic mice with CYP3A inhibitor KET and antioxidant NACA abolishes HS-induced hepatic injury. (A) Schematic representation of the KET and NACA co-treatment model. VP-PXR transgenic mice were pre-treated with KET (95 mg/kg per day) for three days and intraperitoneally injected with NACA one hour before the sham surgery or HS/R. **(B)** Liver histology was analyzed by H&E staining.

Bar is 100 μm. **(C)** Serum levels of ALT. Results are presented as mean ±SE. n=3 for each group. *, $p < 0.05$; **, $p < 0.01$, the comparisons are labeled.

Supplementary Figure 8. Post-hemorrhagic shock treatment of NACA attenuates HS-induced hepatic injury. (A) Schematic representation of the NACA post-HS treatment model. WT mice were intraperitoneally injected with PCN (40 mg/kg) or VEH for two days before receiving the sham surgery or HS/R. NACA (200 mg/kg) or saline was given 2 h after the initiation of HS and before resuscitation. **(B)** Liver histology was analyzed by H&E staining. Bar is 100 μm. **(C-E)** Mice are the same as in (B). Shown are quantification of necrotic areas (C), Suzuki scores (D), and serum levels of ALT (E). Results are presented as mean ±SE. n=3 for each group. *, $p < 0.05$; **, $p < 0.01$, the comparisons are labeled.

Supplementary Figure 9. Ablation of Cyp3a abolishes the sensitizing effect of post-hemorrhagic shock treatment of PCN. (A) Schematic representation of the PCN post-HS treatment model. $Cyp3a^{-/-}$ mice were intraperitoneally injected with PCN (40 mg/kg) 2 h after the initiation of HS and right before resuscitation. **(B)** Liver histology was analyzed by H&E staining. Bar is 100 μm. **(C)** Serum levels of ALT. Results are presented as mean ±SE. n=3 for each group.

Supplementary Figure 10. Effects of post-hemorrhagic shock treatment of SPA70 and KET on HS-induced hepatic injury in humanized mice. (A) Schematic representation of the SPA70/KET post-HS treatment models. Mice were intraperitoneally injected with RIF (10 mg/kg) for three days before receiving the sham surgery or HS/R. SPA70 (150 mg/kg), KET(95

mg/kg), or VEH was administrated either 2-h after the initiation of HS (at 72 h), or 12-h after the initiation of HS (at 84 h). **(B)** Liver histology was analyzed by H&E staining. Bar is 100 μm. **(C-E)** Mice are the same as in (B). Shown are quantification of necrotic areas (C), Suzuki scores (D), and serum levels of ALT (E). **(F)** The hepatic mRNA expression of *CYP3A4* in RIF-treated sham groups. Results are presented as mean ±SE. n=3 for each group. *, $p < 0.05$; **, $p < 0.01$, compared to the VEH group (C and D), or the comparisons are labeled (E and F).

Xie et al., Supplementary Figure 1

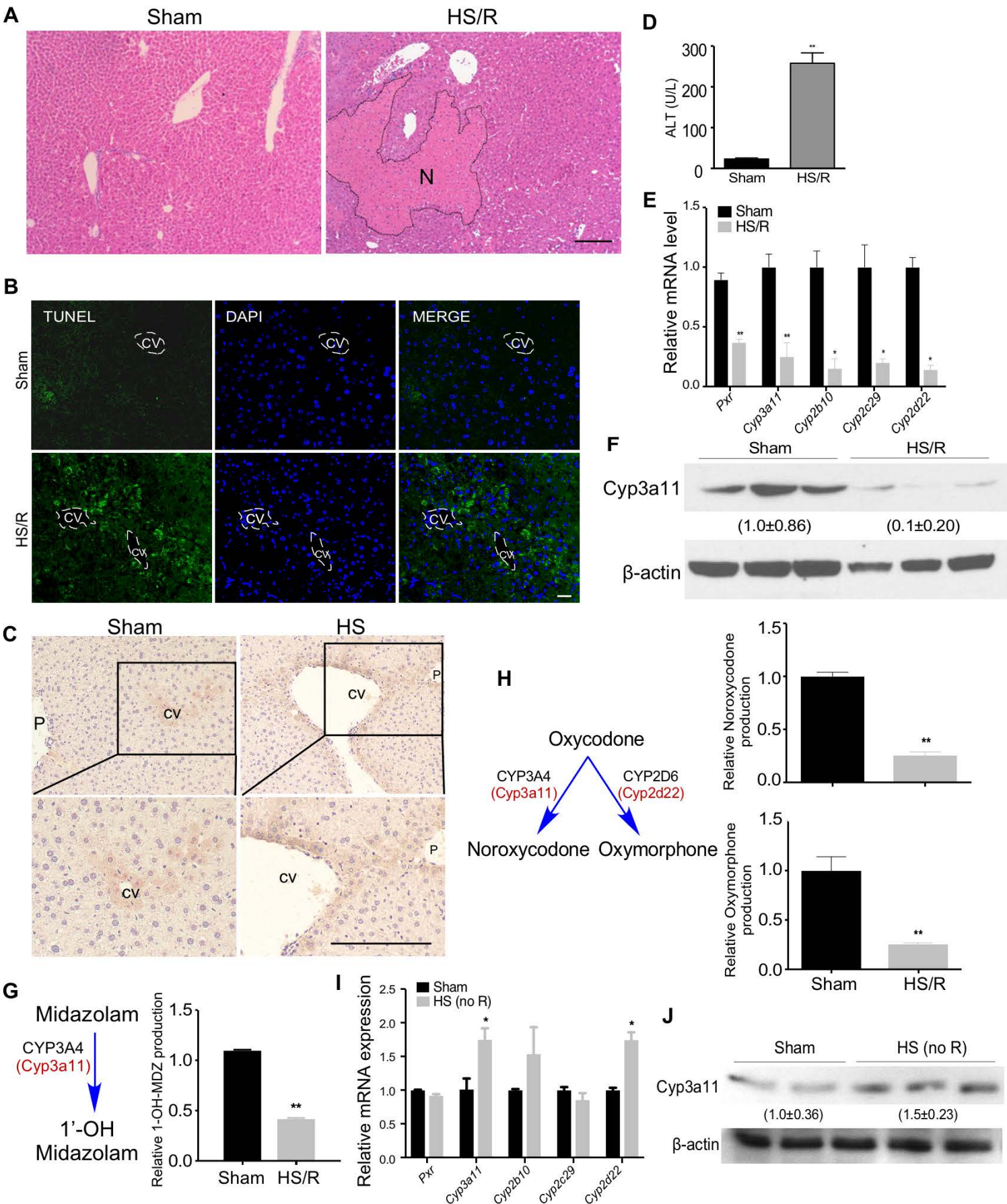

Xie et al., Supplementary Figure 2

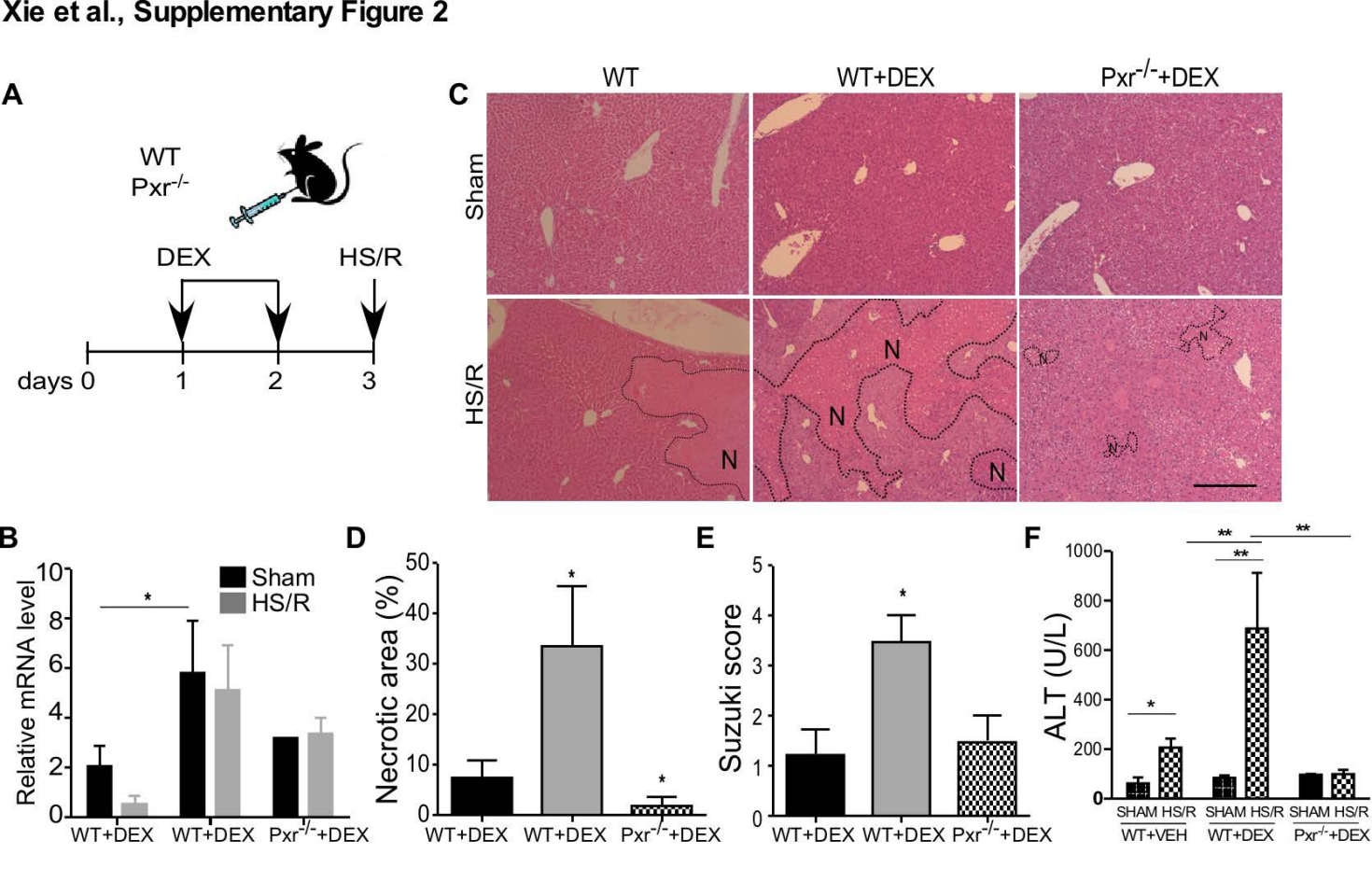

Xie et al., Supplementary Figure 3

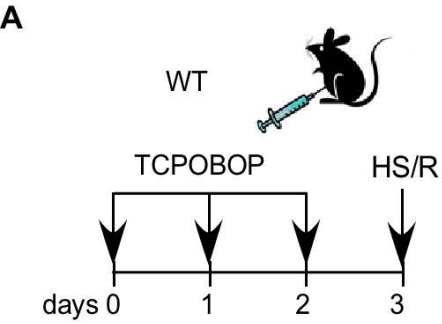

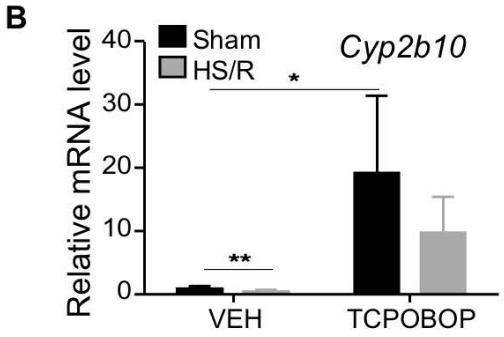

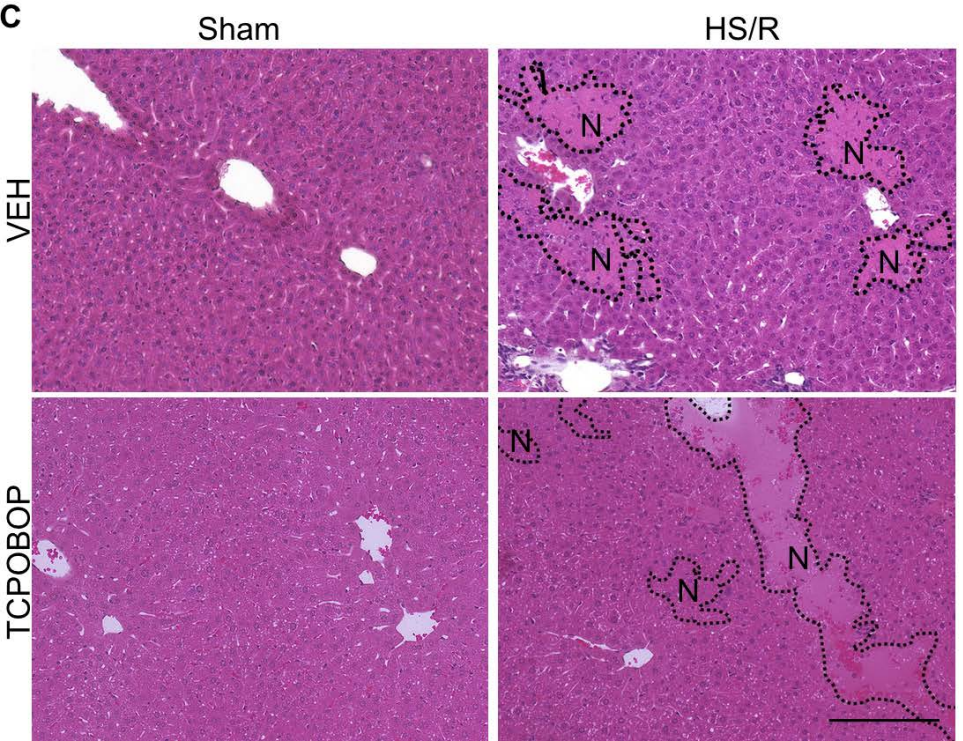

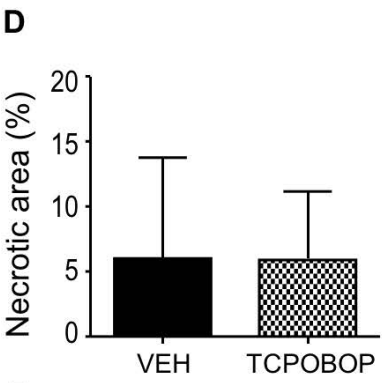

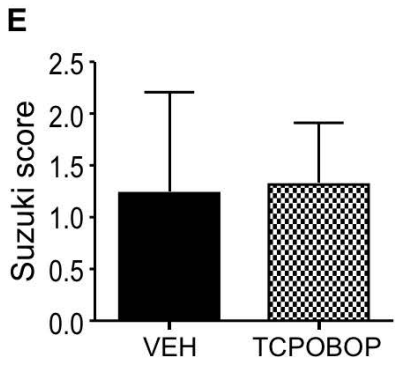

Xie et al., Supplementary Figure 4

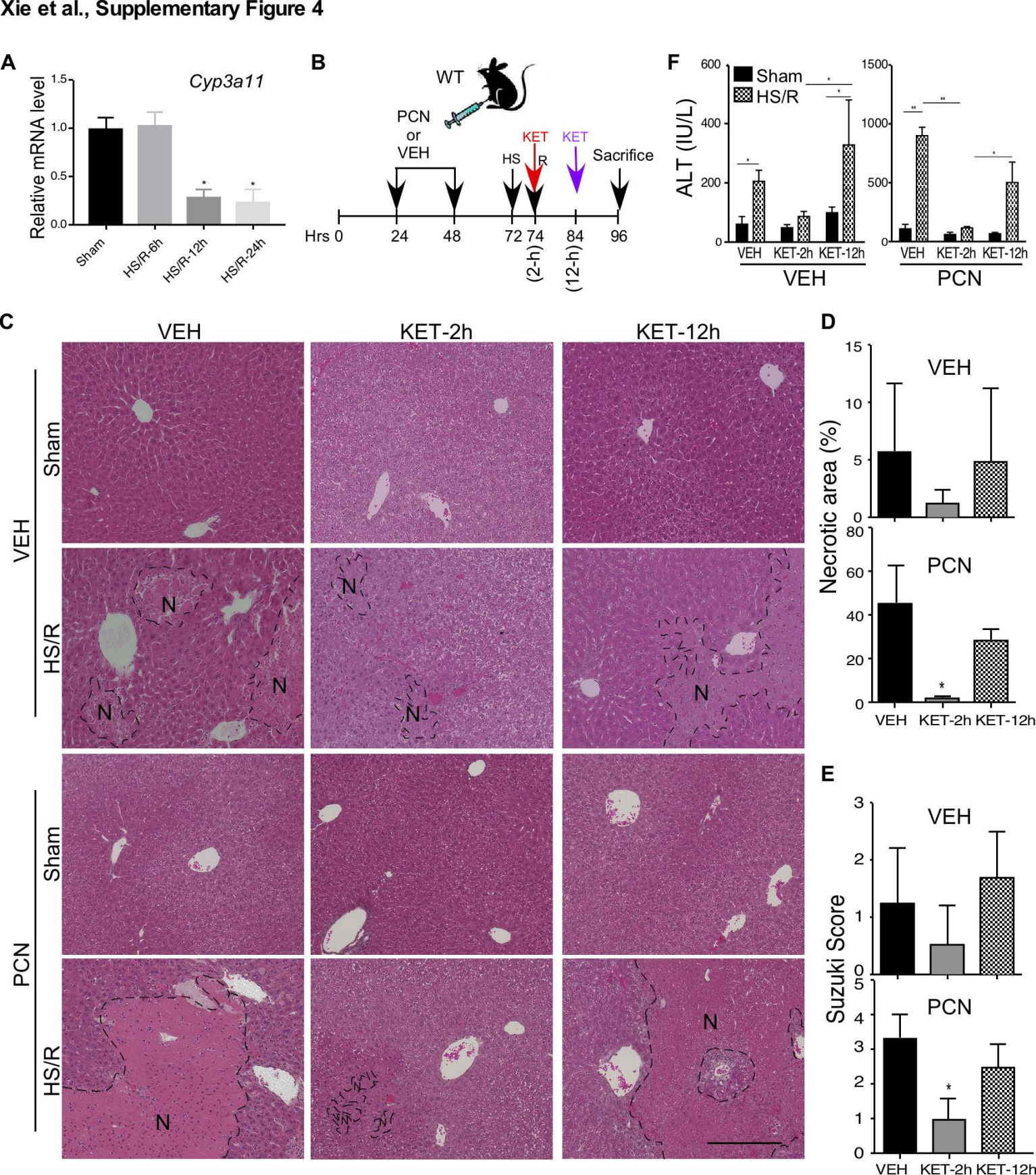

Xie et al., Supplementary Figure 5

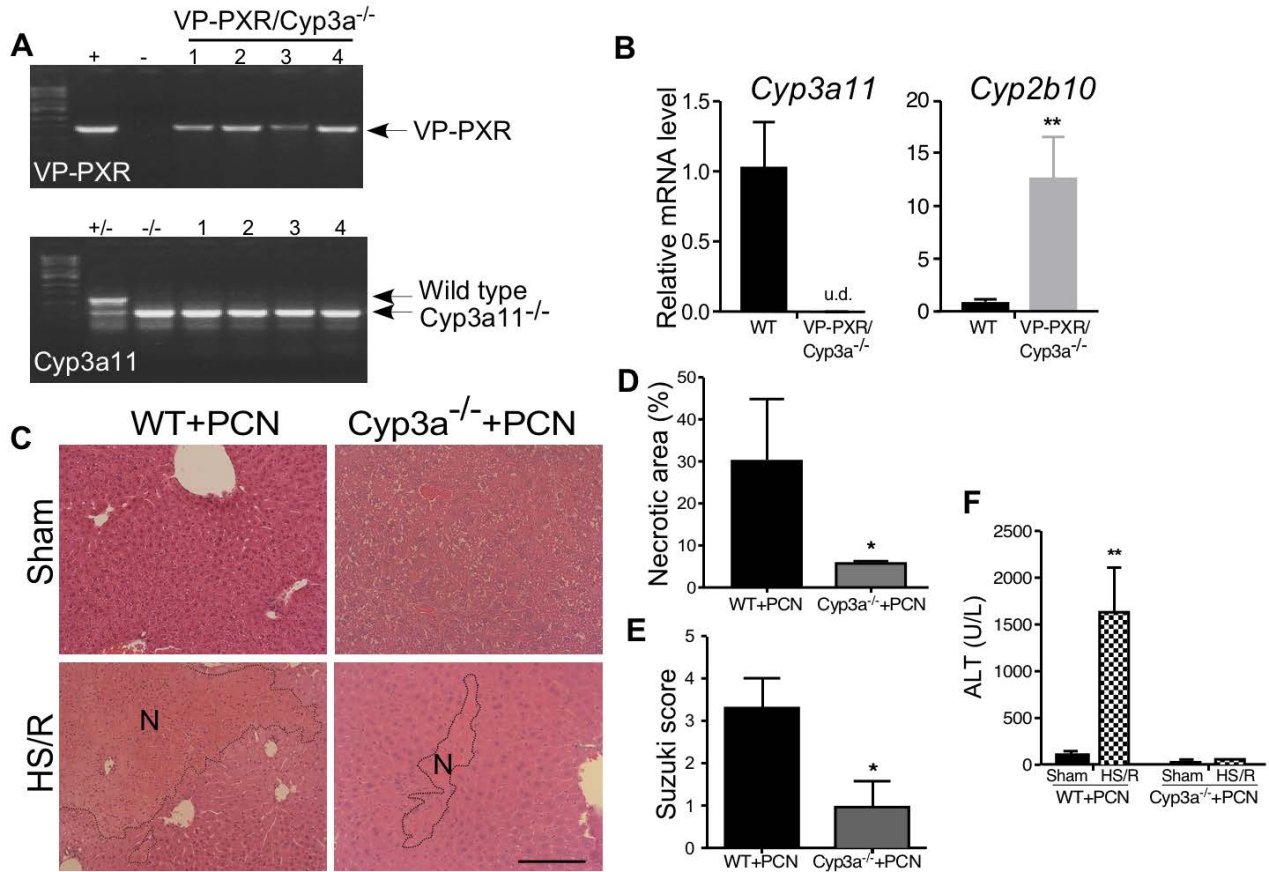

Xie et al., Supplementary Figure 6

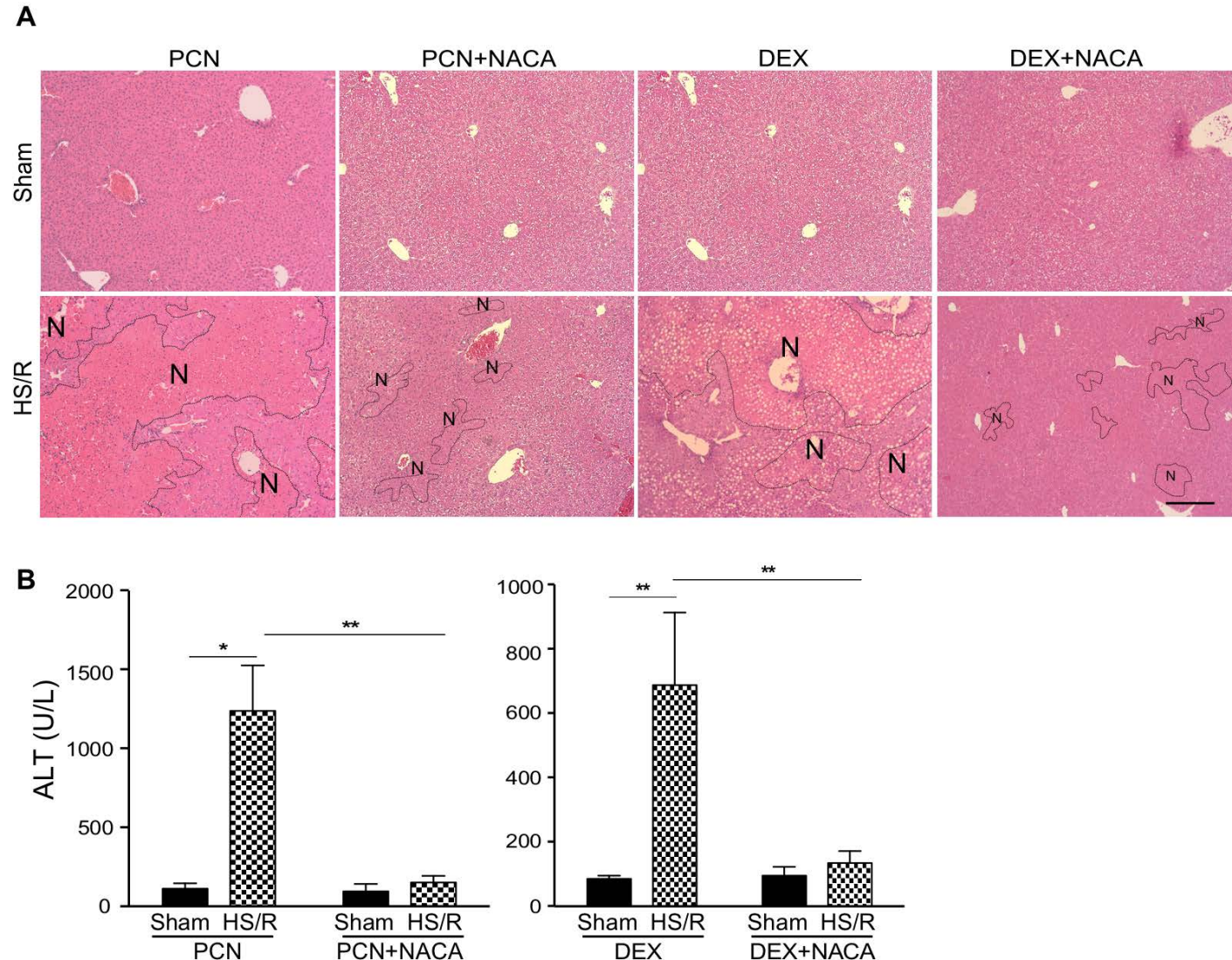

Xie et al., Supplementary Figure 7

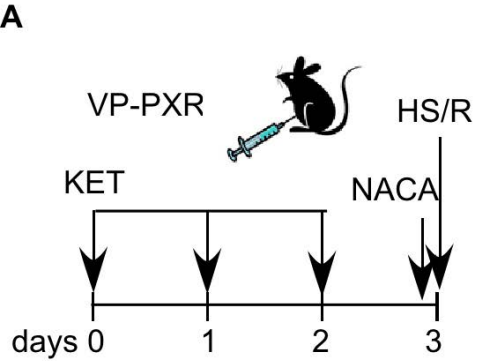

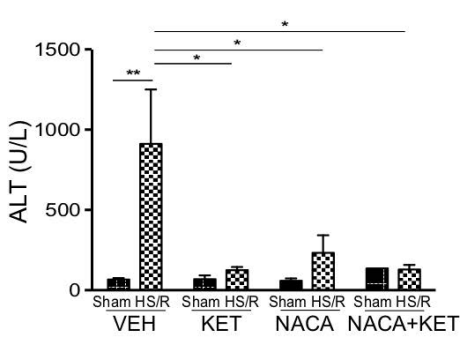

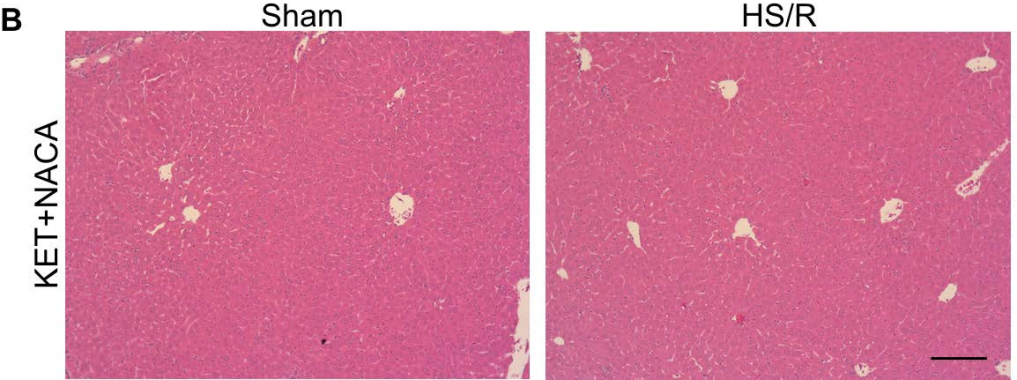

Xie et al., Supplementary Figure 8

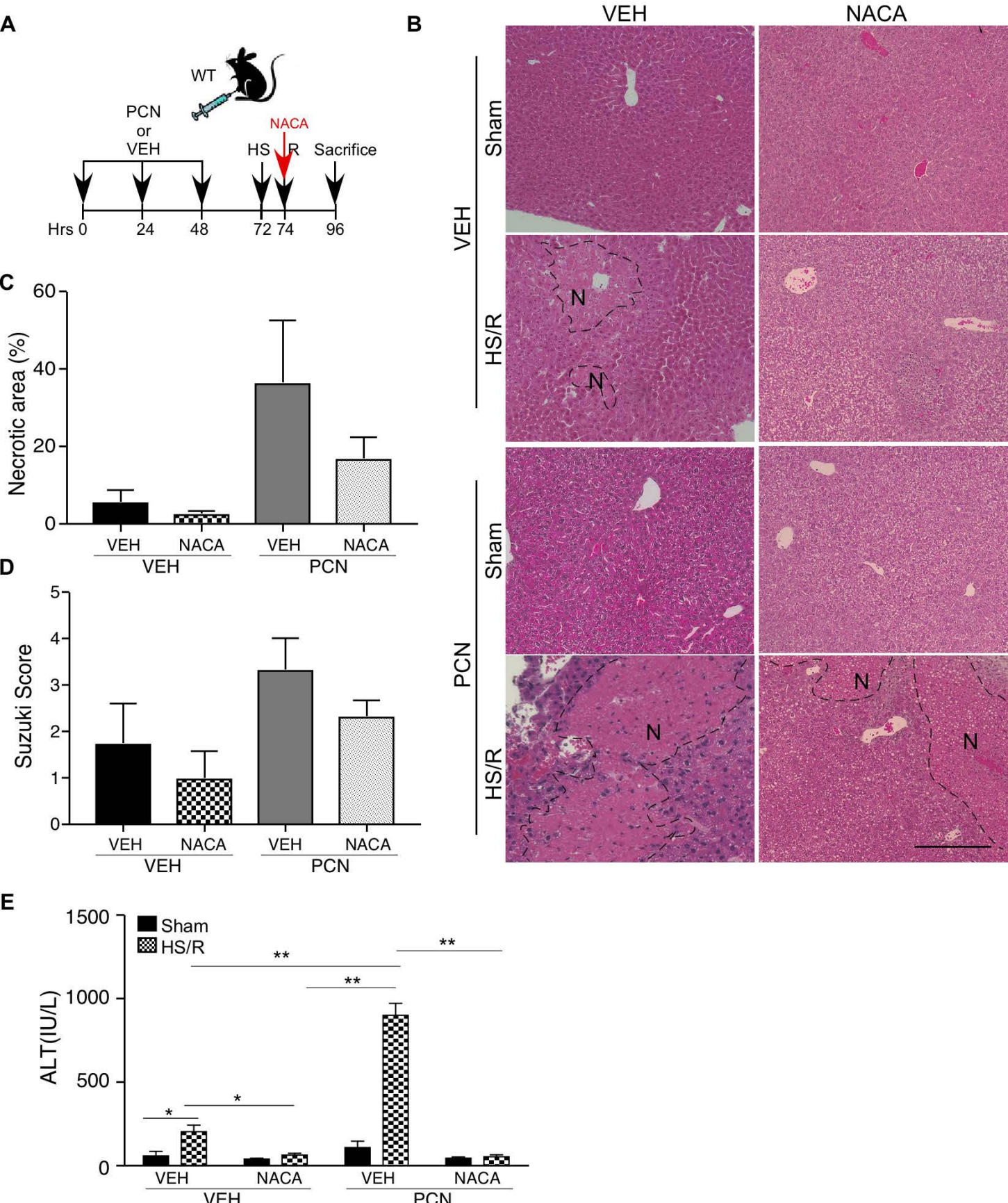

Xie et al., Supplementary Figure 9

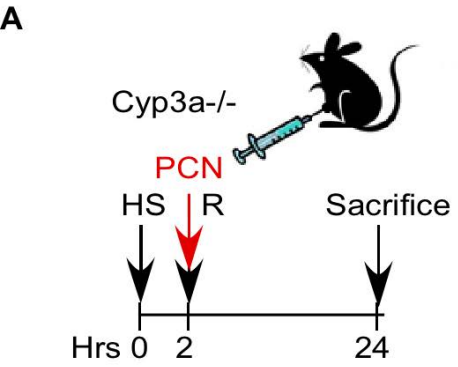

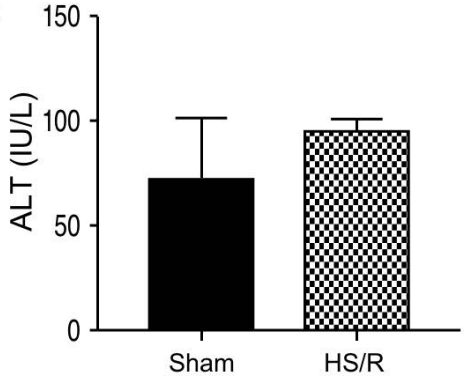

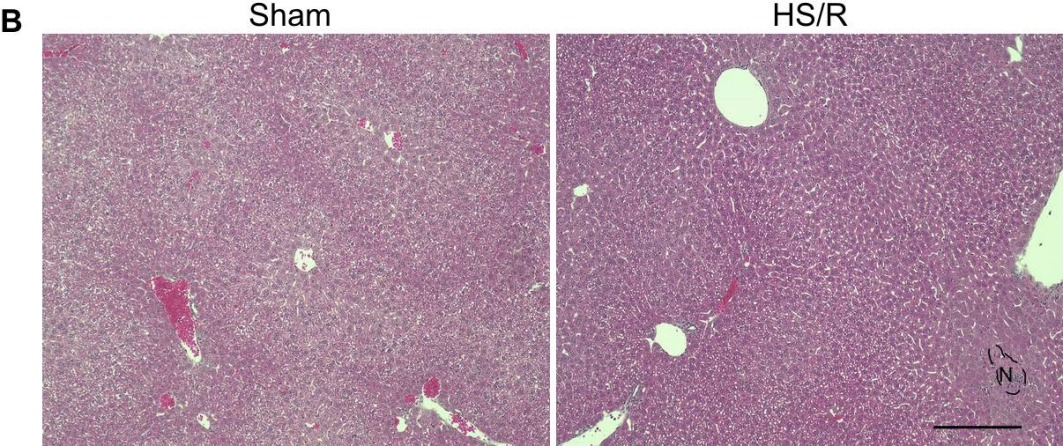

Xie et al., Supplementary Figure 10

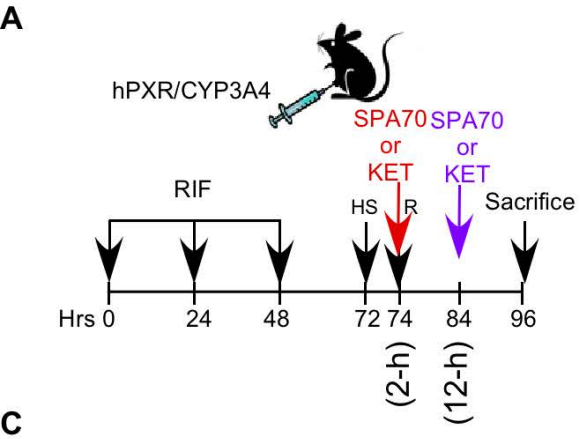

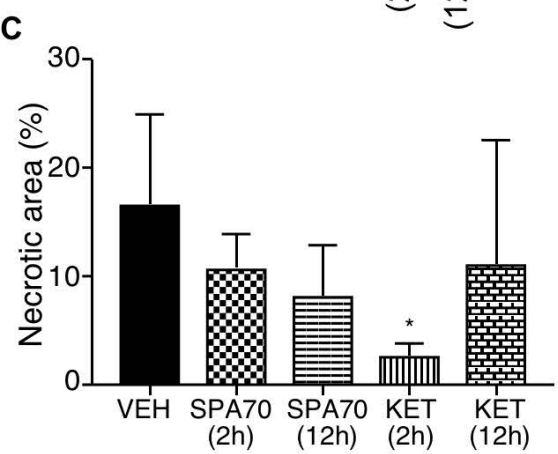

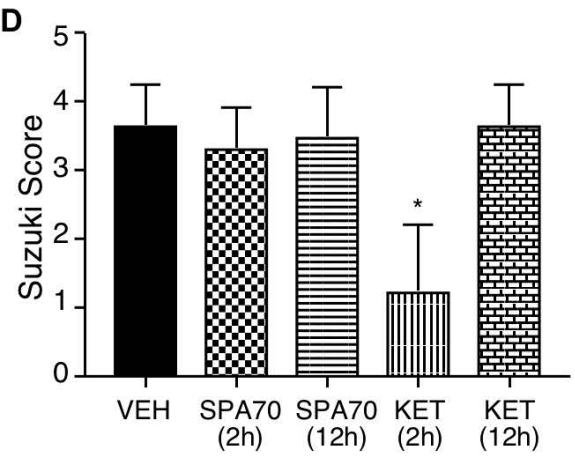

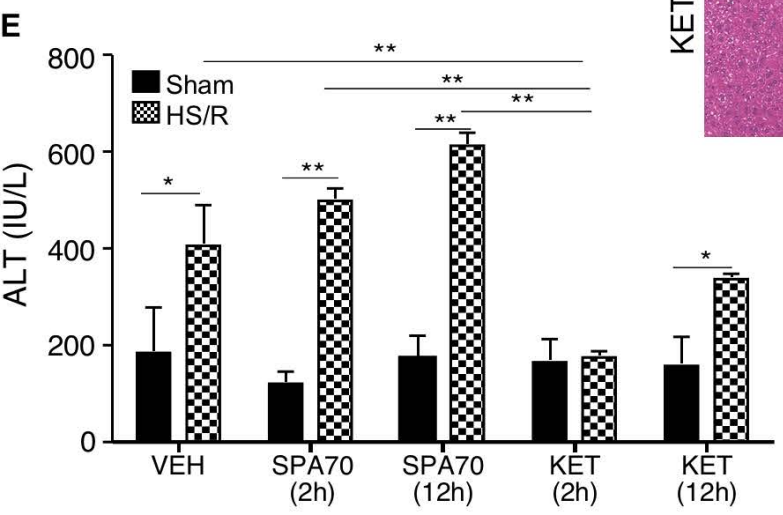

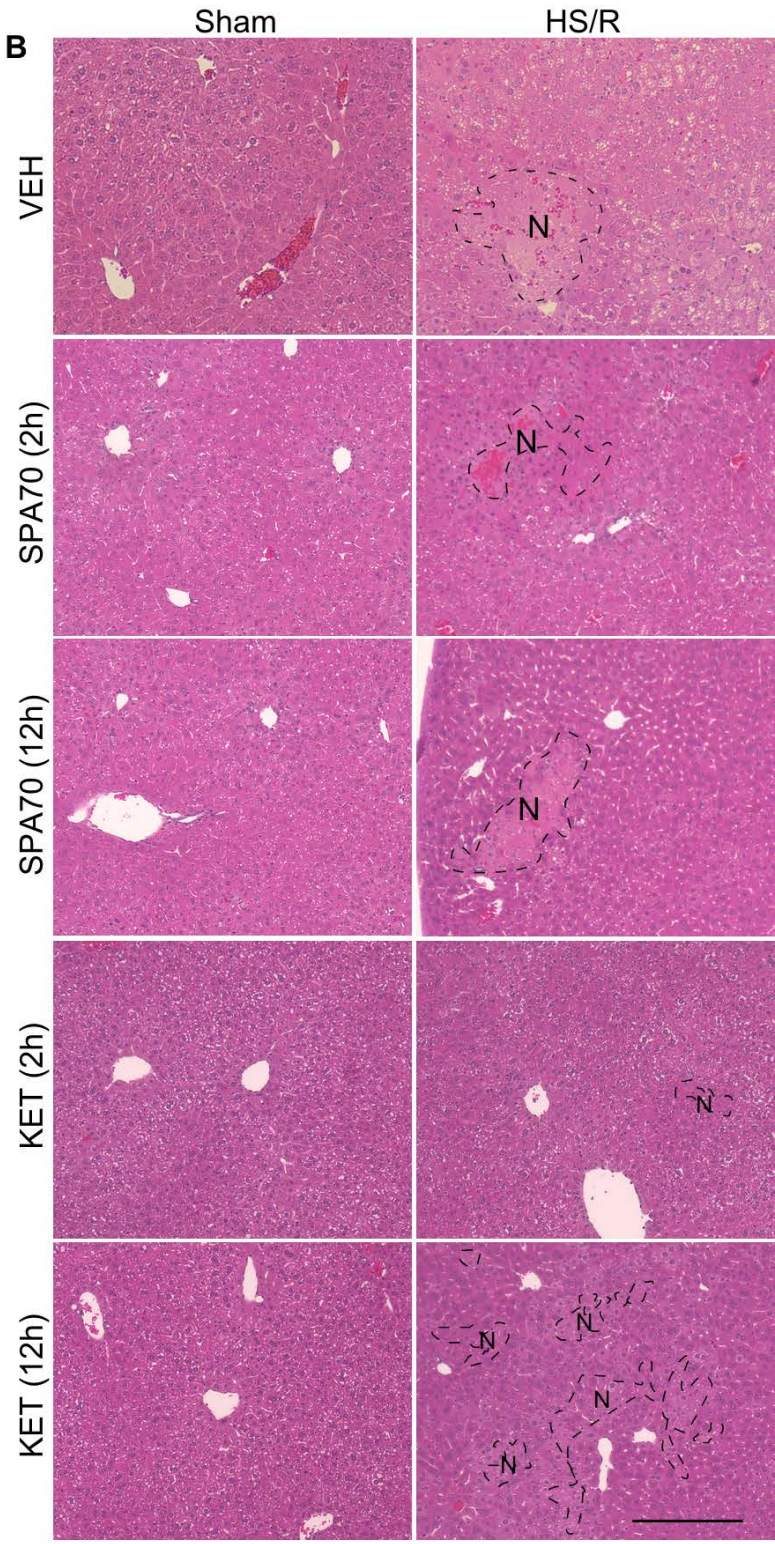

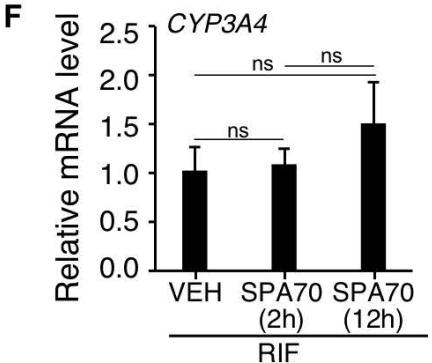

Xie et al., Supplemental Materials and Methods

EXPERIMENTAL PROCEDURES

Chemicals

Ketoconazole (KET), dexamethasone (DEX) and pregnenolone 16α-carbonitrile (PCN) were purchased from Sigma-Aldrich (St. Louis, MO). KET was prepared by dissolution in ethanol and Tween 80 (1:1(v/v)) and then further dilution with saline. SPA70, a gift from Dr. Taosheng Chen (St. Jude Children's Research Hospital), was prepared by dissolution in 30% PEG-400 dissolved in saline.

Histology, Immunohistochemistry, and Immunofluorescence

Five-micron thick paraffin sections were stained with hematoxylin-eosin for general histology. Necrosis was estimated by dividing the necrotic area by the entire histological section using ImageJ software. Sections were scored from 0-4 for sinusoidal congestion, hydropic degeneration, necrosis, neutrophilic infiltration, and steatosis, which were used to calculate the Suzuki score (Suzuki et al., 1993). For 4-hydroxynonenal (4-HNE) immunostaining, liver paraffin sections were incubated with the primary 4-HNE antibody (Ab48506) from Abcam (Cambridge, MA) at 1:25 dilution overnight at 4 °C. The secondary antibody used was anti-mouse monoclonal at 1:500 dilution. The signal was visualized by peroxidase reaction using 3,3′-diaminobenzidine as the chromogen. Hematoxylin was used for nuclear counterstain. At least three mice were used for each treatment group or genotype, and for each sample at least four non-contiguous regions were photographed and analyzed. For 8-hydroxyguanosine (8-OHdG)

immunofluorescence, liver paraffin sections were incubated with primary 8-OHdG antibody (Ab48508) from Abcam at 1:200 dilution overnight at 4 °C. The secondary antibody was a Cy3 (Cyanine 3) conjugated donkey anti-mouse monoclonal at 1:500 dilution. DAPI was used for nuclear counterstain.

Real-time PCR and Western Blot Analysis

Total RNA was treated with RNase-free DNase I and reverse transcribed into single stranded cDNA. Real-time PCR using the SYBR Green-based assay was performed with the ABI 7300 Real-Time PCR System. The real-time PCR primer sequences are provided in Supplementary Tables 1-2. For Western blotting, 20 μg of total protein for each sample were separated on 10% SDS-polyacrylamide gel. The primary antibodies included a monoclonal mouse antibody against 4-HNE (Ab48506, 1:200) and a polyclonal rabbit antibody against Cyp2b10 (Ab9916, 1:200) from Abcam, and a monoclonal mouse antibody against Cyp3a11/CYP3A4 (1:200), which was a gift from Dr. Frank J. Gonzalez (National Cancer Institute, NIH).

Serum Chemistry

Blood samples were collected by cardiac puncture. Serum aminotransferase (ALT) levels were measured using an assay kit from Stanbio (Boerne, TX).

Analysis of Microsomal Metabolism of Midazolam and Oxycodone

Microsomes were prepared from the mouse livers as described (Matsubara et al., 1974). Fifty mg liver tissue was homogenized with buffer A (0.1 M phosphate buffer, pH7.5;

0.25 M sucrose; 0.154 M KCl; 1mM protease inhibitor) and centrifuged at 100,000 g for 25 min at 4 °C. The pellets were washed once with buffer B (0.1 M phosphate buffer, 20% v/v glycerol) and resuspended in 200 µl buffer B. The metabolisms of midazolam and oxycodone were measured by incubating 0.5 mg/ml microsomes with 30 µM midazolam or 0.1 mg/ml microsomes with 300 µM oxycodone in a tube containing 0.1 mM PBS (pH=7.4). The incubation was initiated by adding 1 mM NADPH. After incubation for 10 min at 37 °C for midazolam or 120 min at 37 °C for oxycodone, 100 µl ice-cold methanol was added to stop the reaction. The samples were vortexed for 30 s, then centrifuged at 15000 rpm for 10 min. One hundred µl of supernatant was transferred to an autosampler vial for UPLC-MS analysis. The UPLC-MS analysis was performed as described (Tien et al., 2015; Fang et al., 2013).

References

Suzuki S, Toledo-Pereyra LH, Rodriguez FJ, Cejalvo D. Neutrophil infiltration as an important factor in liver ischemia and reperfusion injury. Modulating effects of FK506 and cyclosporine. Transplantation 1993;55:1265-1272.

Matsubara T, Prough RA, Burke MD, Estabrook RW. The preparation of microsomal fractions of rodent respiratory tract and their characterization. Cancer Res 1974;34:2196-2203.

Tien YC, Liu K, Pope C, Wang P, Ma X, Zhong XB. Dose of Phenobarbital and Age of Treatment at Early Life are Two Key Factors for the Persistent Induction of Cytochrome P450 Enzymes in Adult Mouse Liver. Drug Metab Dispos 2015;43:1938-1945.

Fang WB, Lofwall MR, Walsh SL, Moody DE. Determination of oxycodone, noroxycodone and oxymorphone by high-performance liquid chromatography-electrospray ionization-tandem mass spectrometry in human matrices: in vivo and in vitro applications. J Anal Toxicol 2013;37:337-344.

Supplementary Table 1. Oligonucleotide sequences of primers used for real-time PCR.

Gene Name	NCBI Reference Sequence	Sequences
mCyp3a11	NM_007818.3	Forward: 5'- AGGGAAGCATTGAGGAGGAT -3'
		Reverse: 5'- GGTAGAGGAGCACCAAGCTG -3'
mCyp2b10	NM_009999.4	Forward: 5'- CGCATGGAGAAGGAGAAGTC -3'
		Reverse: 5'- CTCTGCAACATGGGGTACT -3'
mCyp2c29	NM_007815.3	Forward: 5'- CATGCAAGACAGGAGCCACA -3'
		Reverse: 5'- CTGCATCAGGCAGGCTAGTG -3'
mCyp2d22	NM_019823.4	Forward: 5'- GGGCCTTTGTTACCATGTTGG -3'
		Reverse: 5'- TACTCGGCGCTGCACATCTG -3'
mPXR	NM_010936.3	Forward: 5'- GGGATAGGGTTACAGCACGA -3'
		Reverse: 5'- TCTGAAAAACCCCTTGCATC -3'
mCatalase	NM_009804.2	Forward: 5'- CACTGACGAGATGGCACACT-3'
		Reverse: 5'- CACTGACGACGAGATGGCACACT-3'
mSod2	NM_013671.3	Forward: 5'- TCTGTGGGAGTCCAAGGTTC-3'
		Reverse: 5'- TAAGGCCTGTTGTTCCTTGC-3'
mGst-α	NM_008181.3	Forward: 5'- GCAGGGGTGGAGTTTGAAGA-3'
		Reverse: 5'- TCTCTTTGGTCTGGGGGACA-3'
mGst-mu	NM_008183.3	Forward: 5'- TTCCCAATCTGCCCTACTTG-3'
		Reverse: 5'- TGCCATAGCCTGGTTCTCC-3'
mGst-pi	NM_013541.1	Forward: 5'- TGCCACCATACACCATTGTC-3'
		Reverse: 5'- CCAGCCTTGCATCCAGGTAT-3'
mCyclophilin	M60456	Forward: 5'- GGCTCCGTCGTCTTCCTTTT -3'
		Reverse: 5'- TGACACGATGGAACTTGCTGT -3'
hPXR	NM_003889.3	Forward: 5'- ACTCCCCTCACCTGCCATAA -3'
		Reverse: 5'- CTCTTGGACTGCTTGGTGGT -3'
hCYP3A4	NM_017460.5	Forward: 5'-GTCTTTGGGGCCTACAGCAT -3'
		Reverse: 5'- GGGATGAGGAATGGAAAGACTGTT -3'

Supplementary Table 2. Oligonucleotide sequences of primers used for genotyping.

Gene Name	Sequences
hPXR	Forward: 5'-GCA CCT GCT GCT AGG GAA TA-3'
	Reverse: 5'-CTC CAT TGC CCC TCC TAA GT-3'
mPXR	Forward: 5'-CTG GTC ATC ACT GTT GCT GTA CCA-3'
	Reverse-1: 5'- GCA GCA TAG GAC AAG TTA TTC TAG AG -3'
	Reverse-2: 5'-CTA AAG CGC ATG CTC CAG ACT GC -3'
FABP promoter (FABP-VP-PXR)	Forward: 5′-CCATCGATAATTCTCAGAATACAAAACAGT-3′
	Reverse: 5′-CCCAAGCTTCTGACCACAACAGCTCTGTCTGC-3′
Cyp3a11	Forward: 5'-GGTAGCTAGTATAGCAGAACC-3'
	Reverse: 5'-GTACATACAGCTCAGAGCCTG-3'
	Wild-type Cyp3a11 Forward: 5'-CCACCAAATTGACATGAGTCC-3'